

The magnitude of the shift for the new value of curvature radius is inversely proportional to  $R_s$ .

Using Eq. (4) with the measured values of  $\Delta H$  and  $R_s$  yields the value of the radius of curvature of the little spherical protrusion at the [100] direction of Cu as  $K = (0.36 \pm 0.02) \times 10^8 \text{ cm}^{-1}$ . The resonance field for the transition from  $n=1$  to  $m=2$  in the flat-surface geometry from our measurements appears as  $21.4 \pm 0.2$  Oe at a frequency of 35.33 GHz. Combining this with the value of  $K$  as obtained from the curvature-shift determination, we obtain a value of the Fermi velocity at the [100] point as  $1.11 \pm 0.04 \times 10^8 \text{ cm/sec}$ . Values for  $K$  and  $v_F$  can be compared directly with those derived by Shoenberg and Halse from a fitting scheme for de Haas-van Alphen and cyclotron-resonance data.

Shoenberg and Halse<sup>4</sup> give  $K = 0.37 \times 10^8 \text{ cm}^{-1}$  and  $v_F = 1.04 \times 10^8 \text{ cm/sec}$ .

We are led to conclude that the present measurements satisfactorily bear out the expected results for the microwave resonance signals due to bound electron states on curved surfaces. We have illustrated how a measurement of the curvature shift directly yields the Fermi-surface curvature  $K$  and, when combined with the conventional plane-surface data, allows a determination of  $v_F$ . The sensitivity of the resonances to surface curvature provides additional confirmation of the interpretation of the low-field resonances as due to specularly reflected electron states.<sup>2</sup>

<sup>4</sup> M. R. Halse, Ph.D. thesis, Cambridge University, 1967 (unpublished).

## Piezoreflectance of Dilute $\alpha$ -Phase Ag-In Alloys\*

CHARLES E. MORRIS† AND DAVID W. LYNCH

*Institute for Atomic Research and Department of Physics, Iowa State University, Ames, Iowa 50010*

(Received 12 November 1968)

The fractional change in reflectivity due to strain  $\Delta R/R$  of evaporated film samples of four silver-indium alloys was measured in the energy range 2.5–4.5 eV. The films had indium concentrations of 0.4, 1.6, 3.3, and 5.0 at.%. A Kramers-Kronig inversion of  $\Delta R/R$  yielded the change, due to strain, of the phase shift of the reflected electric field. The strain-induced changes of the real and imaginary parts of the complex dielectric constant,  $\Delta \epsilon_1$  and  $\Delta \epsilon_2$ , were calculated. Interpretation of the structure in  $\Delta \epsilon_2$  of silver and the four alloys yielded the following conclusions. (a) The structure in  $\Delta \epsilon_2$  at 4.06 eV in silver is due to the  $L_2' \rightarrow L_1$  (Fermi surface to conduction band) transition and not to the  $L_3 \rightarrow L_2'$  ( $d$  band to Fermi surface) transition as previously suggested. (b) The  $L_2' \rightarrow L_1$  band gap in silver is 4.15 eV and decreases to about 3.7–3.8 eV in the 5.0% indium alloy. (c) Indirect transitions contribute to  $\epsilon_2$  and  $\Delta \epsilon_2$  below the direct  $L_2' \rightarrow L_1$  transition energy in the silver-indium alloys.

### INTRODUCTION

PIEZO-OPTICAL experiments on solids can give useful information when carried out in the region of strong interband absorption. In this range of photon energies the absorption and reflection spectra consist of broad, overlapping structures because at any one photon energy, transitions can occur between several sets of bands or sub-bands. The application of stress causes different regions of the band structure to shift in energy by different amounts. Those transitions between states which are localized in particular regions of wave-vector space exhibit characteristic shifts when various uniaxial or hydrostatic stresses are applied. There also may be shape changes in the spectrum if a uniaxial stress lifts a degeneracy. Coupled with some knowledge of band structures, piezo-optical measurements, especially those using uniaxial stress, enable one to identify the regions of  $\mathbf{k}$  space in which interband transitions are

occurring. This type of experiment has been carried out on Si,<sup>1,2</sup> Ge,<sup>1,2</sup> and Cu<sup>3,4</sup> with considerable success.

Less information can be obtained from piezo-optical measurements on polycrystalline films because one sees only the result of averaging a uniaxial stress or strain over crystal-lattice directions in the sample. Even here, however, one often finds that the piezo-optical response is large only in a small wavelength region. This makes piezo-optical measurements a useful tool for following one interband absorption structure, or several that overlap, as a metal or semiconductor is alloyed. Measurements of the piezoreflectance of evaporated films of the noble metals were made by Engeler *et al.*<sup>5,6</sup>

<sup>1</sup> H. R. Philipp, W. C. Dash, and H. Ehrenreich, Phys. Rev. **127**, 762 (1962).

<sup>2</sup> U. Gerhardt, Phys. Letters **9**, 117 (1964); Phys. Rev. Letters **15**, 401 (1965); Phys. Status Solidi **II**, 801 (1965).

<sup>3</sup> U. Gerhardt, D. Beaglehole, and R. Sandrock, Phys. Rev. Letters **19**, 309 (1967).

<sup>4</sup> U. Gerhardt, Phys. Rev. **172**, 651 (1968).

<sup>5</sup> W. E. Engeler, H. Fritzsche, M. Garfinkel, and J. J. Tiemann, Phys. Rev. Letters **14**, 1069 (1965).

<sup>6</sup> M. Garfinkel, J. J. Tiemann, and W. E. Engeler, Phys. Rev. **148**, 695 (1966); **155**, 1046 (1967).

\* Work performed in the Ames Laboratory of the U. S. Atomic Energy Commission. Contribution No. 2430.

† Present address: Los Alamos Scientific Laboratory, Los Alamos, N. M.

TABLE I. Indium concentrations  $C$  (at.%) and lattice parameters  $a_0$  (Å) of alloy samples.

Starting material		Film	
$C$	$a_0$ (in Å at 0°C)	$C$	$a_0$ (in Å at 0°C)
2.26	4.09253	0.4±0.2	4.08770
3.16	4.09595	1.6±0.2	4.09130
4.82	4.10027	3.3±0.2	4.09592
6.38	4.10297	5.0±0.2	4.10068

Recently Morgan and Lynch<sup>7</sup> (ML) measured the optical constants of dilute  $\alpha$ -phase Ag-In alloys, containing up to 4.1% In. There is a strong interband edge in  $\epsilon_2$  around 3.9 eV in silver, which splits upon alloying. This edge was first believed<sup>8</sup> to be due to the " $L_3 \rightarrow L_2$ " ( $d$  band to the Fermi surface near  $L$ ) transition, but recent reassessments of the situation<sup>9-13</sup> suggest that this transition should be overlapped by weak " $L_2' \rightarrow L_1$ " transitions from the Fermi surface near  $L$  to a higher conduction band. As indium is added to silver, the main part of the edge shifts slowly to higher energy, while a weak peak shifts more rapidly to lower energy and becomes stronger. ML attributed the main edge to  $L_3 \rightarrow L_2'$  transitions and the weak peak to  $L_2' \rightarrow L_1$  transitions, but the location of the  $L_2' \rightarrow L_1$  transition could not be determined in pure silver because of overlap. The rapid shift of the  $L_2' \rightarrow L_1$  transition with solute concentration is a result of the great sensitivity of the  $L_1$  levels to the crystal potential.<sup>14,15</sup> The four degenerate  $L_1$  levels should shift readily under volume stress and split with  $[111]$ -directed uniaxial stress. The  $L_2' \rightarrow L_1$  transitions should thus have a large piezo-optical response, even though they give rise to only "weak" absorption. In fact, as shown below, they completely dominate the piezo-reflectance spectrum of silver, the stronger  $L_3 \rightarrow L_2'$  transition producing negligible piezo-reflectance by comparison.

In the following, we report piezo-reflection measurements on silver and silver-indium alloys. Our results for silver agree with those of Garfinkel, Tiemann, and Engeler<sup>6</sup> (GTE), although our identification of the transition disagrees with theirs. The  $L_2' \rightarrow L_1$  transition

can be followed until the indium concentration reaches about 5%. We obtain a value of 4.15 eV for the  $L_2' \rightarrow L_1$  gap in silver at room temperature and show how this gap shifts upon alloying with indium. Finally, we see a strong piezo-reflectance structure at energies below that of the  $L_2' \rightarrow L_1$  edge. We believe this arises from indirect transitions, with the solute atoms acting as scattering centers, from states on and near the Fermi surface near  $L_2'$  to the higher conduction band near  $L_1$ .

## EXPERIMENTAL METHOD

### Sample Preparation

Silver and indium were fused together by arc melting to make the alloys. Chemical analysis of the alloys showed the indium concentrations varied from 1.21 to 6.38 at.%. The lattice parameters of the alloys were measured to obtain a calibration curve, used in determining the indium concentration of the evaporated samples. The samples were made by evaporating the alloys upon the polished face of a lead zirconate-lead titanate transducer. A deposition was simultaneously made on a glass substrate. It took approximately 120 sec to produce a film about 1  $\mu$ m thick by evaporation from a molybdenum boat. The pressure rose from  $5 \times 10^{-9}$  to  $8 \times 10^{-8}$  Torr during the evaporation.

Since the vapor pressures of indium and silver are slightly different at high temperatures, there was a possibility that the indium concentration of the evaporated film is different from that of the starting material. By measuring the lattice parameter of the sample on the glass substrate, it was possible to determine the indium concentration of the evaporated films. The solute concentrations and lattice parameters of the starting materials and the evaporated films are shown in Table I. The uncertainty in solute concentration in a film is due to the finite widths of the diffraction lines. In order to get sharp x-ray diffraction lines, it was necessary to anneal the films after evaporation. The films were annealed in vacuum at 310°C for 4 h. When the alloys were not annealed, only faint diffraction patterns were obtained, probably because the just-evaporated films were inhomogeneous and strained.

The transducers used to strain the film were 12 mm square and 4 mm thick. They were poled such that when a voltage was applied between the square faces, they expanded (or contracted) uniformly while the thickness decreased (or increased), depending on the polarity of the voltage. The films presumably follow the shape changes of the transducer, although accurate knowledge of the strain is not necessary in what follows.

### Optical Measurements

The experimental apparatus shown in Fig. 1 is similar to that used by GTE, except that  $\Delta R/R$  is not measured directly. Light from a xenon arc was incident

<sup>7</sup> R. M. Morgan and D. W. Lynch, Phys. Rev. **172**, 628 (1968).

<sup>8</sup> H. Ehrenreich and H. R. Philipp, Phys. Rev. **128**, 1622 (1962).

<sup>9</sup> C. N. Berglund and W. E. Spicer, Phys. Rev. **136**, A1044 (1964).

<sup>10</sup> W. F. Krolikowski, Solid State Electronics Laboratory, Stanford Electronics Laboratories, Technical Report No. 5218-1, 1967 (unpublished).

<sup>11</sup> D. Beaglehole, Proc. Phys. Soc. (London) **85**, 1007 (1965); **87**, 461 (1966).

<sup>12</sup> D. Beaglehole, in *Optical Properties and Electronic Structure of Metals and Alloys*, edited by F. Abeles (North-Holland Publishing Co., Amsterdam, 1966), p. 154.

<sup>13</sup> F. M. Mueller and J. C. Phillips, Phys. Rev. **157**, 600 (1967).

<sup>14</sup> F. Herman and S. Skillman, in *Proceedings of the International Conference on Semiconductors, Prague, 1960*, edited by J. Bardeen (Czechoslovakian Academy of Sciences Publishing House, Prague, 1961), p. 20.

<sup>15</sup> J. C. Phillips, Phys. Rev. **125**, 1931 (1962).

on a monochromator with an average bandpass of 0.02 eV. The "unpolarized," collimated beam leaving the monochromator was deflected onto the sample at near normal incidence (angle of incidence less than  $11^\circ$ ) and then onto a photomultiplier with an S-13 response. An oscillator applied a 1.1-kHz voltage to the transducer, which, in turn, applied a uniform planar ac strain of amplitude  $e_{xx}=e_{yy}=4.1 \times 10^{-5}$  to the sample. The beam reaching the detector had a modulated component proportional to the change in the reflectivity  $\Delta R$  of the sample due to strain and a dc component proportional to the reflectivity  $R$  of the unstrained sample. The ac component of the photocurrent was measured synchronously with the strain field by a synchronous amplifier, the dc component was measured by a dc voltmeter, and the outputs of both were recorded. To ensure the proper correlation of the outputs, the time constants of the ac and dc channels were made equal. All measurements were made with samples at room temperature. In this experiment only  $\Delta R/R$  is needed, not the values of  $\Delta R$  or  $R$  separately, so all constants of proportionality cancel out.

A xenon arc was used over the entire wavelength range 2.5–4.5 eV. The power supply for the arc was a well-regulated, low-ripple (0.01%), constant-current supply.

The transducer on which the sample was deposited was held by two Plexiglas supports (see Fig. 1). Leads from the oscillator were glued to the square faces, and printed circuit paint was used to make electrical contact with the electrodes. The sample was mounted at its center of gravity to minimize induced vibrations of the photomultiplier. This mechanical decoupling of the oscillating sample from the photomultiplier was necessary to eliminate spurious signals from induced oscillatory motion of the dynode structure.

There are other unwanted signals, as noted by GTE, which cannot be avoided. The normal vibration of the sample modulates the beam coherently with the signal, even when the optical constants of the sample are strain-independent. Since the beam and the photocathode are nonuniform, an ac signal is produced. Finite beam size and nonuniformities in the optical path and sample surface also inject false signals. It was assumed that these spurious signals merely shift the zero level of  $\Delta R/R$  and do not cause structure. An analytical procedure was used to determine the true zero level.

#### Data Analysis

In order to formulate a piezo-optical experiment and perform the required data analysis, it is necessary to know the effects of strain upon the optical properties of a solid. In general, a cubic solid under strain no longer exhibits isotropic optical properties. The tensor properties of the strain and complex dielectric constant tensor need to be considered. GTE showed that evaporated noble-metal films under a uniform planar strain

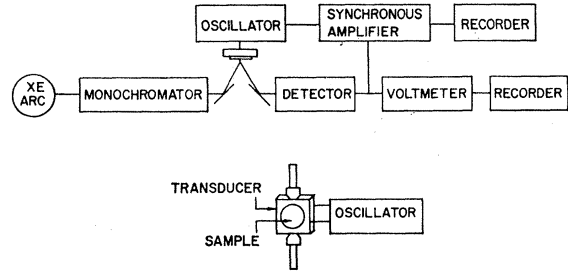


FIG. 1. Schematic diagram of (a) the experimental setup, (b) the sample holder.

could be characterized by a scalar complex dielectric constant in the expansion plane. Their evaporated films consisted of crystallites having either a  $\langle 111 \rangle$  or a  $\langle 100 \rangle$  axis normal to the plane of the film, otherwise being randomly oriented. Since the evaporated alloy films in this experiment are assumed to have the same structure, the tensor properties of  $\epsilon_1$  and  $\epsilon_2$  can be ignored in the data analysis.

In a piezoreflection experiment the fractional change in reflectivity due to strain  $\Delta R/R$  is measured. In order to extract information about the band structure from the experiment, one must relate  $\Delta R/R$  to  $\Delta \epsilon_1$  and  $\Delta \epsilon_2$ , the strain-induced changes in the real and imaginary parts of the dielectric constant, respectively. The equations needed to relate  $\Delta R/R$  to  $\Delta \epsilon_1$  and  $\Delta \epsilon_2$  are given by GTE. Briefly, one finds  $\Delta \theta$ , the strain induced change of the phase shift of the electric field upon reflection, by a dispersion integral on  $\Delta R/R$ . One needs to "extrapolate"  $\Delta R/R$  to zero and infinite photon energies. From  $\Delta R/R$  and  $\Delta \theta$ , straightforward algebra yields

$$\Delta \epsilon_1 = [n(\epsilon_1 - 1) - k\epsilon_2] \frac{1}{2} \Delta R/R + [k(\epsilon_1 - 1) + n\epsilon_2] \Delta \theta, \quad (1)$$

$$\Delta \epsilon_2 = [k(\epsilon_1 - 1) + n\epsilon_2] \frac{1}{2} \Delta R/R - [n(\epsilon_1 - 1) - k\epsilon_2] \Delta \theta, \quad (2)$$

where the complex dielectric constant  $\tilde{\epsilon} = \epsilon_1 - i\epsilon_2$  is related to the complex refractive index  $\tilde{N} = n - ik$  by  $\tilde{N}^2 = \tilde{\epsilon}$ . To obtain extrapolated values of  $\Delta R/R$  at photon energies below the lowest used, GTE used

$$\frac{\Delta \epsilon_2}{\epsilon_2} = \left[ -1 + \frac{1 - \omega^2 \tau^2}{1 + \omega^2 \tau^2} \left( \frac{2}{3} \frac{d \ln r}{d \ln V} \right) \right] \frac{\Delta V}{V} \quad (3)$$

and

$$\frac{\Delta \epsilon_1}{\epsilon_1 - 1} = \left[ -1 + \frac{2}{1 + \omega^2 \tau^2} \left( \frac{2}{3} \frac{d \ln r}{d \ln V} \right) \right] \frac{\Delta V}{V}. \quad (4)$$

These describe the changes in  $\epsilon_1$  and  $\epsilon_2$  produced in a free-electron gas by the volume change  $\Delta V$ . Shear strain should have no effect on  $\tilde{\epsilon}$  for a free-electron gas.  $r$  is the dc resistance of a film of free-electron gas with relaxation time  $\tau$ . GTE ignored the second term in square brackets in Eq. (4). This is justified if  $\omega\tau \gg 1$ , a condition which is satisfied in the data region 2.5–4.5 eV, but not in the energy region below 2.5 eV, where  $\Delta R/R$  is being extrapolated. We used Eq. (4) as written

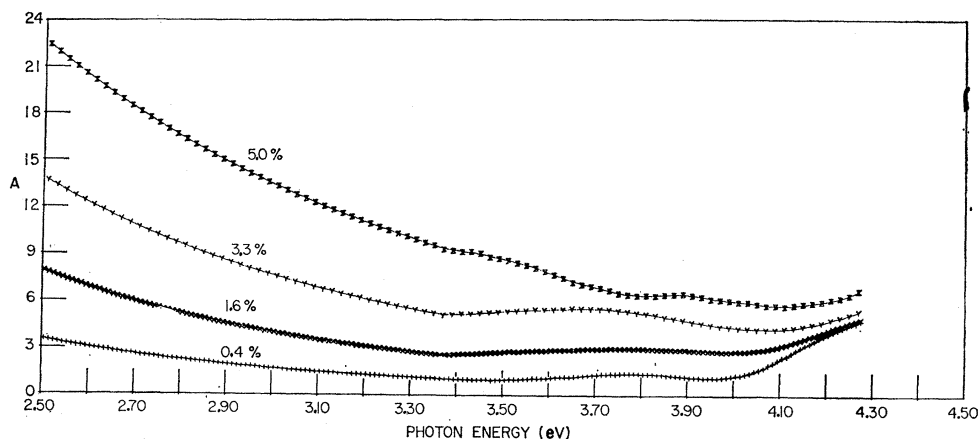


FIG. 2. — $A$  for silver-indium alloys [see Eqs. (1), (2), (10), (11)].

with  $\Delta V/V$  set equal to twice the linear strain of the transducer. Equations (3) and (4) and Drude expressions for  $\bar{\epsilon}$  gave  $\Delta R/R$  for photon energies below 2.5 eV. The zero level of  $\Delta R/R$  in the region 2.5–4.5 eV was adjusted to make the data join smoothly with the calculated  $\Delta R/R$  at 2.5 eV.

To extrapolate  $\Delta R/R$  in the high-energy region ( $>4.5$  eV),  $\Delta R/R$  was set equal to a constant, the experimental value at 4.5 eV. GTE extrapolated  $\Delta R/R$  in the high-energy region so that the calculated values of  $\Delta\theta$ , using the dispersion integral, equaled the free-carrier values of  $\Delta\theta$  in the low-energy region. When the extrapolation technique of GTE was tried for the three most dilute alloys, the calculated  $\Delta\theta$  agreed with that calculated using the simpler extrapolation, except for a slight zero shift. For the most concentrated alloy, the contribution to  $\Delta\theta$ , in the 2.5–4.5-eV interval, of the integral over  $\Delta R/R$  in the high-energy region dominated the contribution due to the other two regions, giving an unphysical result. It does not seem reasonable that a small increase in indium concentration would introduce a large (compared to the other alloys) change in  $\Delta R/R$  in the high-energy region, especially when the trend in the data region was to reduce  $\Delta R/R$  substantially. Because of this, we chose the aforementioned high-energy extrapolation.

The values of  $\tau$ ,  $\omega_p$ , and  $d \ln r/d \ln V$  must be specified for the alloys before  $\Delta\theta$  can be calculated. Matthiessen's rule was used to estimate  $\tau$ . Matthiessen's rule states<sup>16</sup> that

$$\frac{1}{\tau} = \frac{1}{\tau_L} + \frac{1}{\tau_I} + \frac{1}{\tau_J} \quad (5)$$

for dilute alloys with nonmagnetic impurities, i.e., that the reciprocals of the relaxation times of the various electron scattering processes are additive. The first term on the right-hand side represents the frequency

of scattering by phonons, the second term represents the frequency of scattering by impurities, and the third represents the frequency of scattering by other mechanisms, such as grain boundaries, vacancies, and strains. For dilute alloys ( $<5\%$ ) it was assumed the first and third terms were constant, independent of indium concentration, and equal to the reciprocal of the relaxation time of a pure silver film. The second term was assumed to be proportional to the indium concentration. According to ML, the sum of the first and third terms equals  $0.175 \times 10^{15} \text{ sec}^{-1}$  for silver films prepared the same way our alloy films were made. The proportionality constant in the second term is  $0.0308 \times 10^{15} \text{ sec}^{-1}$  and was determined from Linde's<sup>17</sup> resistivity data on silver-indium alloys. The experimental value of  $d \ln r/d \ln V$  for pure silver, 3.6, was determined by Lawson.<sup>18</sup> Since the bulk resistivity  $\rho$  is proportional to  $\tau^{-1}$ , the bulk resistivity of an alloy can be written

$$\rho = \rho_L + \rho_I + \rho_J, \quad (6)$$

and the resistance can be written

$$r = r_L + r_I + r_J. \quad (7)$$

With the help of Eqs. (5)–(7), straightforward differentiation of  $d \ln r/d \ln V$  yields

$$\frac{d \ln r}{d \ln V} = \frac{\tau_L^{-1} + \tau_J^{-1}}{\tau^{-1}} \frac{d \ln(r_L + r_J)}{d \ln V} + \frac{\tau_I^{-1}}{\tau^{-1}} \frac{d \ln r_I}{d \ln V}. \quad (8)$$

$d \ln(r_L + r_J)/d \ln V$  is equal to  $d \ln r/d \ln V$  for pure silver. The relative values of  $d \ln(r_L + r_J)/d \ln V$  and  $d \ln r_I/d \ln V$  can be approximated from the data of Dugdale and Gugan,<sup>19</sup> which give  $d \ln r/d P$  as a function of temperature for copper. Near  $0^\circ\text{K}$ ,  $d \ln r/d P$  involves only impurity scattering, since  $r_L + r_J \ll r_I$ . At room temperature  $d \ln r/d P$  involves only scattering by

<sup>17</sup> J. O. Linde, *Ann. Physik* **14**, 353 (1932).

<sup>18</sup> A. W. Lawson, *Progr. Metal Phys.* **6**, 1 (1956).

<sup>19</sup> J. S. Dugdale and D. Gugan, *Proc. Roy. Soc. (London)* **A241**, 397 (1957).

<sup>16</sup> J. M. Ziman, *Electrons and Phonons* (Clarendon Press, Oxford, England, 1963).

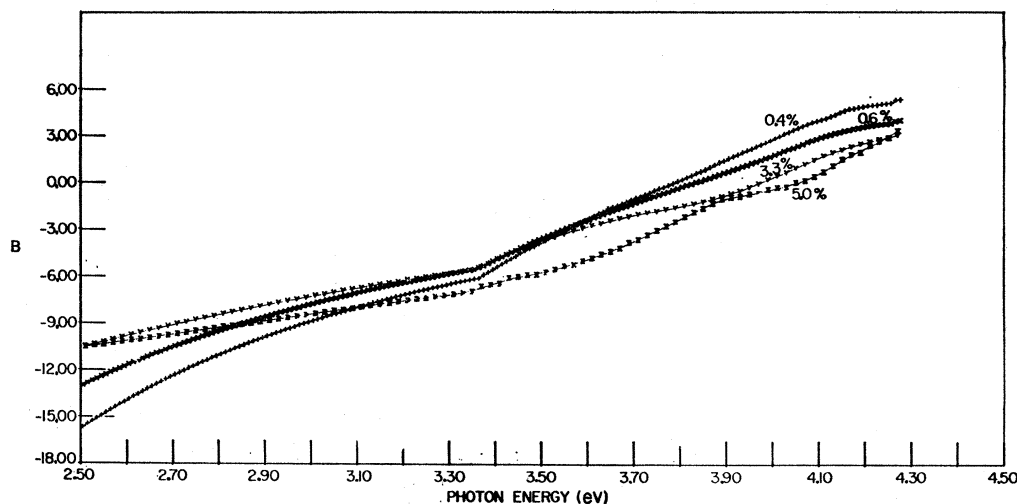


FIG. 3.  $B$  for silver-indium alloys [see Eqs. (1), (2), (10), (11)].

phonons because  $r_L + r_I \gg r_I$  for reasonably pure copper (less than 0.01% impurities).  $d \ln r / d \ln V$  is related to  $d \ln r / dP$  by

$$\frac{d \ln r}{d \ln V} = -B \frac{d \ln r}{dP}, \quad (9)$$

where  $B$  is the bulk modulus. The ratio  $d \ln(r_L + r_I) / d \ln V$  to  $d \ln r_I / d \ln V$  is equal to the ratio of  $d \ln r / dP$  at high and at low temperature if the scattering in silver is the same as in copper and the bulk modulus is not a function of temperature. The latter is a good approximation because the bulk modulus of all the noble metals varies less than 6% between 300 and 0°K.<sup>20,21</sup> The value of  $d \ln r_I / d \ln V$  can now be determined, and is equal to  $-1.1$ . The values of  $\omega_p$ ,  $\tau$  [needed to get  $\Delta \epsilon_1$  and  $\Delta \epsilon_2$  from Eqs. (3) and (4)], and  $d \ln R / d \ln V$  for the alloys are listed in Table II. We obtain the plasma frequency  $\omega_p$  by assuming that each indium atom provides three conduction electrons to the alloy.

To calculate  $\Delta \epsilon_1$  and  $\Delta \epsilon_2$  at a given energy, the values of  $n$  and  $k$  (hence  $\epsilon_1$  and  $\epsilon_2$ ) must be known, in addition to  $\Delta R / R$  and  $\Delta \theta$ . ML have measured the  $n$  and  $k$  values of dilute silver-indium alloys in the energy range 3.35–4.28 eV. The indium concentrations in these alloys were 0.5, 1.0, 1.7, 2.4, and 4.1%.  $n$  and  $k$  values for our alloys of different composition were found by interpolation, using a quadratic least-squares fit of  $n$  and  $k$  as a function of concentration at a fixed energy. The values of  $n$  and  $k$  for the alloys used in this experiment were determined from the fitted curves. In the energy range 2.50–3.35 eV,  $n$  and  $k$  values were calculated from the Drude expressions for  $\epsilon_1$  and  $\epsilon_2$ , since there were not experimental data available. If the

<sup>20</sup> J. R. Neighbours and G. A. Alers, Phys. Rev. **111**, 707 (1958).

<sup>21</sup> W. C. Overton, Jr., and J. Gaffney, Phys. Rev. **98**, 969 (1955).

values of  $\omega_p$  and  $\tau$  given in Table II are used in this region, the  $n$  and  $k$  values do not join smoothly at 3.35 eV with those interpolated from the data of ML. This results from the presence of interband absorption near 3.35 eV. Slightly different  $\omega_p$  and  $\tau$  values were then chosen to effect a smoother junction with the data of ML.

Straightforward evaluation of Eqs. (1) and (2) yielded  $\Delta \epsilon_1$  and  $\Delta \epsilon_2$ . They can be rewritten

$$\Delta \epsilon_1 = A \frac{1}{2} \Delta R / R + B \Delta \theta, \quad (10)$$

$$\Delta \epsilon_2 = B \frac{1}{2} \Delta R / R - A \Delta \theta. \quad (11)$$

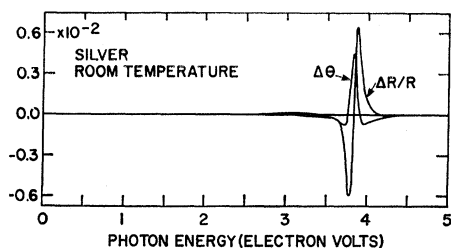
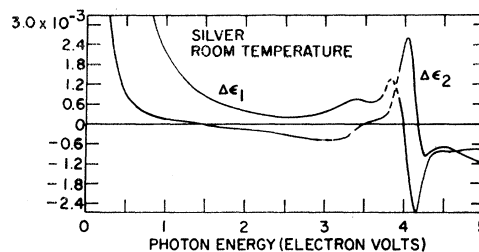
The coefficients  $A$  and  $B$  are shown in Figs. 2 and 3. They are devoid of sharp structure.

## RESULTS AND DISCUSSION

GTE measured the piezoreflection of the noble metals from 1.5 to 5.0 eV. A uniform planar expansion of  $7.0 \times 10^{-5}$  was applied to their films. In the present work the piezoreflection spectra of several silver films were measured in the energy range 2.5–4.5 eV. The results obtained agreed with those of GTE to within 15%. Figure 4 shows their  $\Delta R / R$  and  $\Delta \theta$  spectra for a silver film. The corresponding  $\Delta \epsilon_1$  and  $\Delta \epsilon_2$  for this film are presented in Fig. 5. The data of GTE have been multiplied by a factor of 0.6 to make their data, obtained with larger ac strains, comparable with ours.

TABLE II. Alloy parameters.

Alloy	$\omega_p$ ( $10^{16}$ sec $^{-1}$ )	$\tau$ ( $10^{-15}$ sec)	$\frac{d \ln r}{d \ln V}$
0.4	1.40	5.34	3.29
1.6	1.42	4.46	2.50
3.3	1.44	3.61	1.84
5.0	1.46	3.04	1.40

FIG. 4.  $\Delta R/R$  and  $\Delta\theta$  for silver from Ref. 6.FIG. 5.  $\Delta\epsilon_1$  and  $\Delta\epsilon_2$  for silver from Ref. 6.

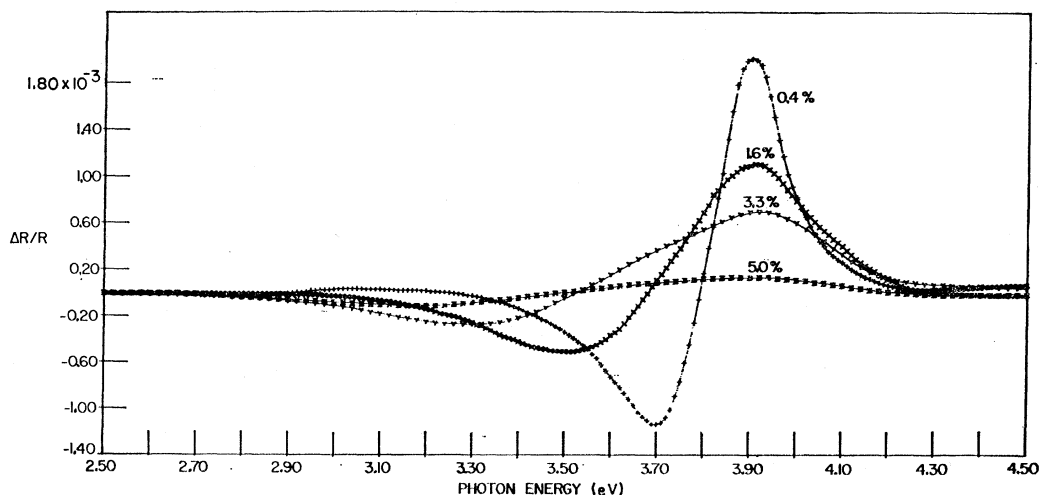
In Figs. 6 and 7, the spectra of  $\Delta R/R$  and  $\Delta\theta$  for four dilute silver-indium alloys are shown. In order of increasing indium concentration, the zero-level corrections to the experimental  $\Delta R/R$  curves were  $4.76 \times 10^{-4}$ ,  $-1.83 \times 10^{-4}$ ,  $1.20 \times 10^{-4}$ , and  $-2.53 \times 10^{-5}$ . The  $\Delta R/R$  spectra display a systematic variation with indium concentration. The structure broadens and shifts to lower energy as the indium concentration is increased. In the 5.0% alloy, the structure has almost disappeared. Since  $\Delta\theta$  is related to  $\Delta R/R$  by a dispersion integral,  $\Delta\theta$  exhibits a similar systematic variation, as in Fig. 7. The structure in  $\Delta R/R$  and  $\Delta\theta$  for pure silver (Fig. 4) is much larger and more localized than that of even the most dilute alloy.

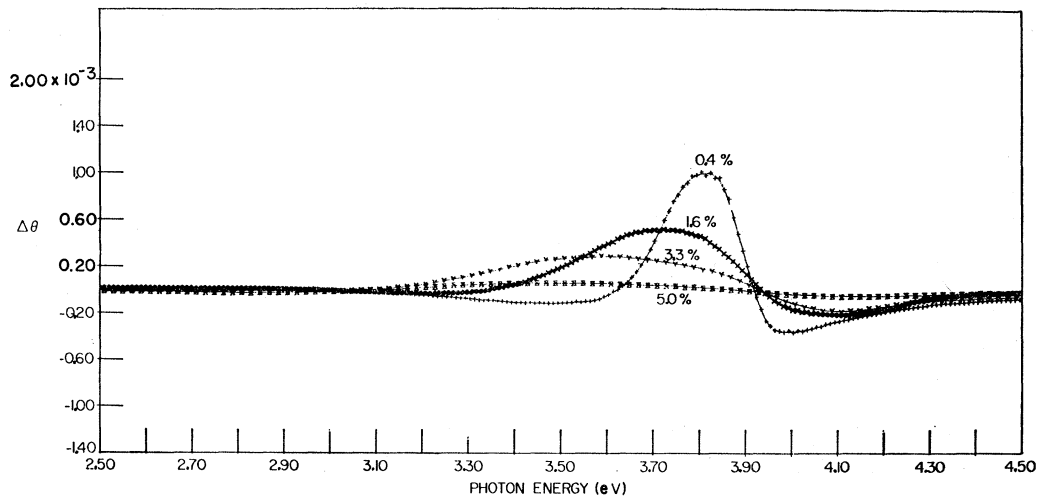
$\Delta\epsilon_1$  and  $\Delta\epsilon_2$  are shown in Figs. 8 and 9. There is a systematic variation of  $\Delta\epsilon_2$  from the 0.4% alloy to the more concentrated ones, except for the alloy of highest concentration. The whole curve for this alloy seems to be shifted rigidly downward. The reason for this is probably that the 5.0% alloy is appreciably out of the concentration range (0.5–4.1%) of the alloys of ML, so the extrapolated values of  $n$  and  $k$  are probably in error. Moreover, because the  $\Delta R/R$  spectrum is nearly structureless, the calculation of  $\Delta\theta$  is more dependent on the extrapolations than for the other alloys. It will be assumed, however, that the gross features of this curve are qualitatively correct.

From 2.50 to 3.35 eV, “free-electron” values of  $n$  and  $k$  were used. The alloys are probably not free-electron-like in this region. ML showed that interband absorption took place at 3.35 eV in alloys with 1% indium or greater. There is evidence presented below that indirect interband transitions occur below 3.35 eV, especially in the alloys of highest indium content. Moreover, the slopes of  $A$  and  $B$  are not continuous at 3.35 eV. The  $\Delta\epsilon_1$  and  $\Delta\epsilon_2$  spectra should be treated with some caution below 3.35 eV.

Unlike the structure in  $\Delta R/R$  and  $\Delta\theta$ , which varies radically in magnitude between alloys, the structure in  $\Delta\epsilon_1$  and  $\Delta\epsilon_2$  (Figs. 8 and 9) has the same magnitude for silver and all four alloys. Since  $\Delta\epsilon_2$  is most directly related to any changes in critical points in the joint density of states and to changes in optical matrix elements, an interpretation of the interband transitions should be made in terms of  $\Delta\epsilon_2$ , not  $\Delta R/R$ .

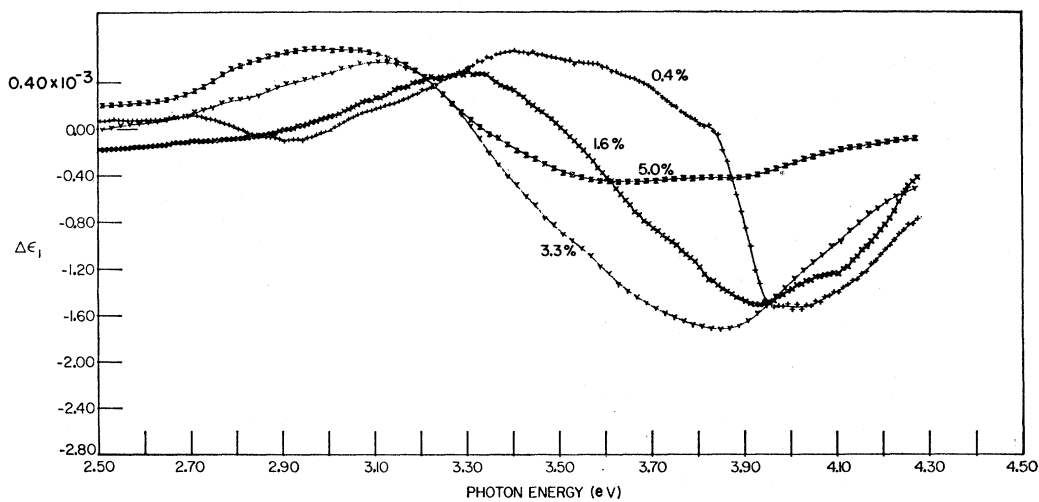
The free-electron contribution to  $\Delta\epsilon_2$  is given by Eq. (3) and will be denoted by  $\Delta\epsilon_2^f$ . A calculation of  $\Delta\epsilon_2^f$  for the various alloys was made with the appropriate values of  $\omega_p$ ,  $\tau$ , and  $d \ln r / d \ln V$ . It was found that the contribution of  $\Delta\epsilon_2^f$  to  $\Delta\epsilon_2$  in the energy range 2.5–4.5 eV is negligible and will be ignored. The structure in  $\Delta\epsilon_2$  arises from  $\Delta\epsilon_2^b$ , the change in  $\epsilon_2^b$ , the interband contribution to  $\epsilon_2$ , due to strain.

FIG. 6.  $\Delta R/R$  for silver-indium alloys.

FIG. 7.  $\Delta\theta$  for silver-indium alloys.

As mentioned previously, ML found upon alloying silver with indium that the strong structure in  $\epsilon_2$  moved to higher energy, while weak structure developed and moved to lower energy. They attributed the weak structure to the  $L_{2'} \rightarrow L_1$  transition and the strong structure to the  $L_3 \rightarrow L_{2'}$  transition. The structure in  $\Delta\epsilon_2$  moves to lower energy in a manner similar to the weak structure in  $\epsilon_2$ . The structure in  $\Delta\epsilon_2$  does not split into two components with increasing indium concentration as occurred in  $\epsilon_2$ . We attribute the structure in  $\Delta\epsilon_2$  to the  $L_{2'} \rightarrow L_1$  transition and not the  $L_3 \rightarrow L_{2'}$  transition assumed by GTE. There are several reasons for this assignment. Since the piezoreflectance effect is due to the modulation of the band structure by the applied stress, it is expected that the dominant structure

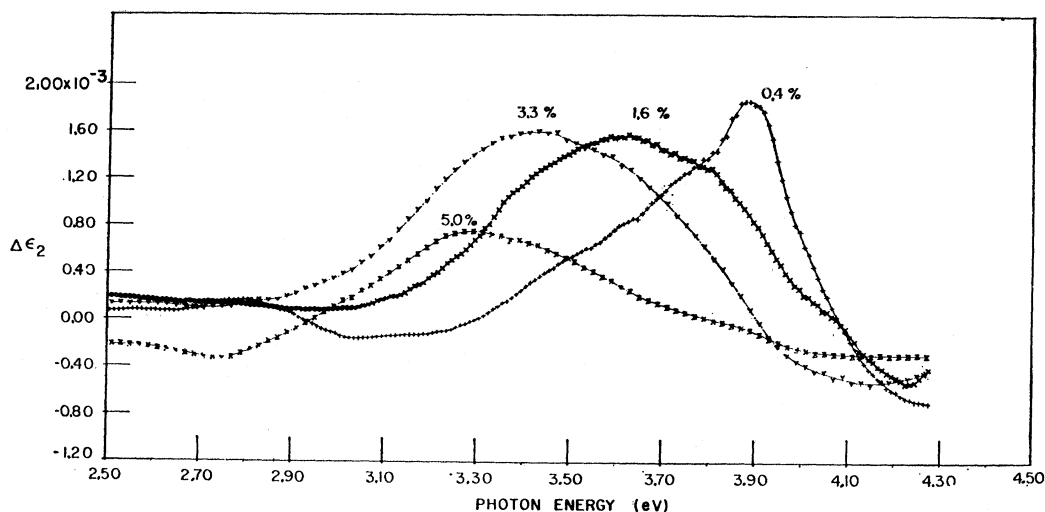
in  $\Delta\epsilon_2$  will be due to interband transitions between energy levels localized in  $k$  space, at least one of which is quite strain-sensitive. Phillips<sup>15</sup> and Herman and Skillman<sup>14</sup> have found that the  $L_1$  level is very sensitive to what crystal potential is used to calculate the energy bands in fcc semiconductors. Band-structure calculations on copper by Segall<sup>22</sup> and by Burdick,<sup>23</sup> using different methods, agreed quite well with regard to the  $L_3$  ( $d$ -like) level and the  $L_{2'}$  ( $p$ -like) level, but differed by more than 1.0 eV for the  $L_1$  ( $s$ -like) level. Thus, in noble metals too, the  $L_1$  level is sensitive to the crystalline potential. Experimentally this was shown to be true by Zallen<sup>24</sup> and by Gerhardt.<sup>4</sup> Zallen found in copper that the  $L_{2'} \rightarrow L_1$  transition was at least seven times more sensitive to hydrostatic pressure than the

FIG. 8.  $\Delta\epsilon_1$  for silver-indium alloys.

<sup>22</sup> B. Segall, *Phys. Rev.* **125**, 109 (1962).

<sup>23</sup> G. A. Burdick, *Phys. Rev.* **129**, 138 (1963).

<sup>24</sup> R. Zallen, in *Optical Properties and Electronic Structure of Metals and Alloys*, edited by F. Abeles (North-Holland Publishing Co., Amsterdam, 1966), p. 164.

FIG. 9.  $\Delta\epsilon_2$  for silver-indium alloys.

$L_3 \rightarrow L_{2'}$  transition. Gerhardt found the  $L_{2'} \rightarrow L_1$  transition in copper to be very sensitive to shear strain as well. Zallen found that the 3.9-eV reflectivity edge in silver had a hydrostatic pressure coefficient at least 2.7 times that of the  $L_3 \rightarrow L_{2'}$  transition in copper. The 3.9-eV edge in silver was at that time attributed to the  $L_3 \rightarrow L_{2'}$  transition, but one expects the  $L_3 \rightarrow L_{2'}$  transition in all noble metals to have similar pressure dependences. Therefore, it appears that more than one transition contributes to the edge in silver, and that the weak  $L_{2'} \rightarrow L_1$  transition, with its presumably larger pressure coefficient, makes a non-negligible contribution to the 3.9-eV edge. ML found that the transition they identified as  $L_{2'} \rightarrow L_1$  shifted by more than 0.5 eV with the 4.1% indium alloy, whereas the strong  $L_3 \rightarrow L_{2'}$  transition shifted less than 0.3 eV. This further supports the correctness of their identification of the transitions because dilute alloying perturbs the crystal potential of the solvent, and one would expect the "sensitive" level to shift more with alloying. In conclusion, the identification of the structure in  $\Delta\epsilon_2$  as arising from the weak  $L_{2'} \rightarrow L_1$  transition seems justified even though the strong  $L_3 \rightarrow L_{2'}$  transition is present.

In discussing the structure in  $\Delta\epsilon_2$  it is convenient to have a tentative band structure for silver and the alloys. Figure 10 is a modified band structure of silver for the first and second conduction bands. The energy gap at  $L$  was set equal to 4.15 eV. The other relevant band parameters are from Refs. 9, 25, and 26. The curvature of the second conduction band was estimated from Segall's<sup>27</sup> band calculation of silver using Hartree-

Fock free-ion functions. It was found to have a curvature roughly equal to three-fourths that of the first conduction band. Because of the relative curvatures of the two bands, a direct transition from the Fermi surface occurs at a lower energy than direct transitions from  $L_{2'}$ . The lowest possible interband transition between the first and second conduction bands would be an indirect transition from the Fermi surface to  $L_1$  at about 3.85 eV.

To a first approximation, the change in  $\epsilon_2$  due to strain is

$$\Delta\epsilon_2(E) = -(\partial\epsilon_2/\partial E)\Delta E, \quad (12)$$

where  $\Delta E$  is the relative shift of a pair of localized regions in  $k$  space. [We use a negative sign here, although Refs. 4 and 6 do not. If  $\Delta\epsilon_2 = \epsilon_2(\text{strain}) - \epsilon_2(\text{no strain})$ , the negative sign is necessary in a derivative experiment (see Fig. 11). The deformation potentials of Refs. 4 and 6 have the correct signs, however.]  $\epsilon_2$  can be written as  $\epsilon_2(E) = A(E)|M(E)|^2g(E)$ , where  $A = 4\pi e^2\hbar^2/m^2E^2$ ,  $M(E)$  is the interband matrix element, and  $g(E)$  is the joint density of states between the two localized regions of  $k$  space, including the Fermi distribution functions. Both  $M$  and  $g$  depend on strain, but we expect that near critical points, the strain-induced relative motion of energy bands, which causes the critical points to shift to new values of  $E$ , will be the dominant effect. Thus we let  $A$  and  $M$  be constant, so that

$$\Delta\epsilon_2(E) = -A|M|^2(\partial g(E)/\partial E)\Delta E. \quad (13)$$

If transitions from more than one pair of bands contribute to  $\epsilon_2$  in a particular range of  $E$ , one must sum over all pairs of bands involved.

The large peak at 4.06 eV in silver is attributed to transitions near the  $L_{2'} \rightarrow L_1$  interband critical point, an  $M_2$  type of critical point.  $g(E)$  is zero for values of  $E$  more than about 0.1 eV below that of the interband

<sup>25</sup> E. Haga and H. Okamoto, J. Phys. Soc. Japan **20**, 1610 (1965).

<sup>26</sup> B. R. Cooper, H. Ehrenreich, and H. R. Philipp, Phys. Rev. **138**, A494 (1964).

<sup>27</sup> B. Segall, Phys. Rev. **125**, 109 (1962); General Electric Research Laboratories Report No. 61-R1 (2785G), 1961 (unpublished).

critical point because the initial states for the corresponding transitions are unoccupied. Actually, this cutoff is about  $kT$  broad.  $g(E)$  then rises rapidly, as the Fermi function approaches unity, then slowly, to a cusplike maximum at the critical point, as shown schematically in Fig. 11(a). If now the  $L_1$  band is shifted lower in energy by dilatation<sup>3,4,24</sup> and positive shear strain,<sup>4</sup> the structure in  $g(E)$  shifts to lower energy, as shown in Fig. 11(a). The difference is shown in Fig. 11(b), and the expected signal from the experiment should resemble this curve, if broadening were included properly. The cutoff of occupied initial states at the Fermi surface causes the first large, positive peak in  $\Delta g/\Delta E$  and the  $M_2$  critical point, the negative. Whether, in fact,  $g(E)$  is increasing just below the critical point [as shown in Fig. 11(a)] or decreasing is not important because it affects only the small section of  $\Delta g/\Delta E$  between the two peaks, a region not detected because of broadening, and the relative heights of the two peaks, a feature also affected by broadening. The structure in Fig. 11(b) is similar to that observed (Figs. 5 and 9) if one ignores the additional low-energy structure. We identify the  $L_{2'} \rightarrow L_1$  gap with the zero between the two peaks, 4.15 eV for pure silver.

Three conspicuous trends are apparent in the  $\Delta\epsilon_2$  spectra (Figs. 5 and 9) as silver is alloyed with indium: (a) The whole structure shifts to lower energy, (b) the structure on the low-energy side of the sharp peak in silver (which will be denoted as low-energy structure) increases with alloying, and (c) the sharp peak at 4.06 eV in pure silver decreases with alloying till it is smaller than the low-energy structure. It also shifts to lower photon energy.

The decrease in this peak ( $L_{2'} \rightarrow L_1$ ) with increasing indium concentration is attributed to increasing diffuseness of the Fermi surface. The blurring of the Fermi surface is a direct result of the uncertainty principle and finite mean free path of the conduction electrons. For example, a mean free path of 100 lattice spacings would imply a 1% uncertainty in the diameter of the Fermi surface. As indium is added, the mean free path at the Fermi surface decreases with a corresponding decrease in the sharpness of the Fermi surface. Another important effect which can decrease and broaden the peak with increasing indium concentration is the increase in the interband relaxation time. ML found considerable broadening in  $\epsilon_2$  with increasing indium concentration.

The low-energy structure in  $\Delta\epsilon_2$  for pure silver extends down to 3.25 eV. This structure cannot be explained by known interband transitions. Low-energy structure also appears in the spectra of the 0.4 and 1.6% alloys. Joos and Klopfer,<sup>28</sup> Huebner *et al.*,<sup>29</sup> Green,<sup>30</sup> and ML

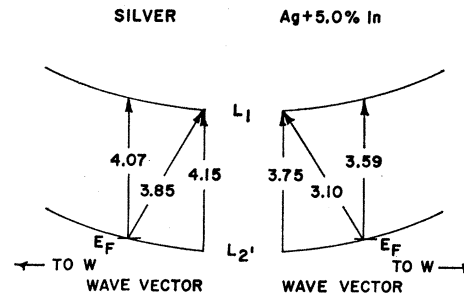


FIG. 10. Band structure near  $L$  for silver and Ag+5 at.% In. All energies are in eV. The Fermi energies are 0.30 and 0.65 eV above  $L_{2'}$  in silver and the alloy, respectively.

have seen a weak peak in  $\epsilon_2$  centered around 3.5 eV in silver. It does not seem to be related to interband transitions because all of the above references find peaks of varying magnitude. This probably indicates that the peak is a surface property. Stanford *et al.*<sup>31</sup> and Dobberstein *et al.*<sup>32</sup> have shown that the magnitude of the peak is related to surface roughness. They found that rougher surfaces produced larger peaks. They attributed this peak to the excitation of nonradiative surface plasmons<sup>33</sup> by photons incident on a rough surface. The samples used in this experiment were relatively rough, having an rms roughness of about 70 Å. (The irregularity of an interference fringe in the thickness-measuring interferometer was used as a measure of the surface roughness.) The structure in  $\epsilon_2$  centered at 3.5 eV might be correlated with the low-energy structure in  $\Delta\epsilon_2$ .<sup>34</sup> If so, then the  $\epsilon_2$  and  $\Delta\epsilon_2$  spectra in this region are misleading, for the magnitude of the structure is not related to the bulk dielectric response function  $\tilde{\epsilon}$ . This effect is better examined in the  $R$  and  $\Delta R/R$  spectra.

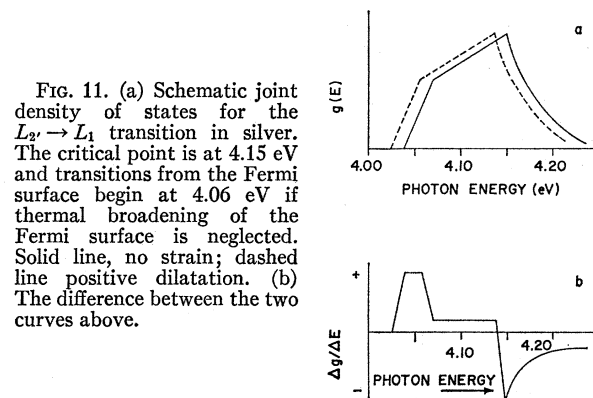


FIG. 11. (a) Schematic joint density of states for the  $L_{2'} \rightarrow L_1$  transition in silver. The critical point is at 4.15 eV and transitions from the Fermi surface begin at 4.06 eV if thermal broadening of the Fermi surface is neglected. Solid line, no strain; dashed line positive dilatation. (b) The difference between the two curves above.

<sup>31</sup> J. L. Stanford, H. E. Bennett, J. M. Bennett, E. J. Ashley, and E. T. Arakawa, *Bull. Am. Phys. Soc. Ser. II*, **13**, 989 (1968).

<sup>32</sup> P. Dobberstein, A. Hamp, and G. Sauerbrey, *Phys. Letters* **27A**, 256 (1968).

<sup>33</sup> H. Raether, *Springer Tracts in Modern Physics* (Springer-Verlag, Berlin, 1965), Vol. 38, p. 84, and references therein.

<sup>34</sup> Silver films evaporated on polished transducers exhibit a large, sample-dependent drop in the reflectivity at about 3.5 eV, while such a drop is not evident in silver films on polished quartz substrates [B. F. Schmidt (private communication)].

<sup>28</sup> G. Joos and A. Klopfer, *Z. Physik* **138**, 251 (1954).

<sup>29</sup> R. H. Huebner, E. T. Arakawa, R. N. Hamm, and R. A. MacRea, *J. Opt. Soc. Am.* **54**, 1434 (1964).

<sup>30</sup> E. L. Green, Ph.D. thesis, Temple University, 1965, University Microfilms No. 66-652 (unpublished).

In fact, a Kramers-Kronig analysis of  $R$  or  $\Delta R/R$  spectra will give erroneous results unless surface effects are first subtracted. Such effects are, however, very small in  $\Delta R/R$  of silver, and structure in the same spectral region probably has a different explanation in our alloys. Examining  $\Delta R/R$  (Fig. 4) around 3.5 eV is difficult. An enlarged plot is given in Fig. 5 of GTE. Superimposed on the tail of the large, rapidly varying negative  $\Delta R/R$  peak of the first interband transition, there is a weak positive structure, beginning below 3.0 eV and peaking near 3.3 eV. The peak value is  $\sim 1.2 \times 10^{-4}$  for a strain of  $4.1 \times 10^{-5}$ . Fedders<sup>35</sup> has calculated the integrated enhanced reflectivity of rough surfaces, but this information is not directly applicable to a derivative experiment. We may assume that the enhanced reflectivity spectrum at a rough surface is proportional to the probability of exciting a surface plasmon,<sup>33</sup>  $P(E) \sim -\text{Im}\{1/[\bar{\epsilon}(E)-1]\}$ . This has a sharp peak at the surface plasmon frequency 3.6 eV. As a first approximation, this function shifts rigidly to lower energy by  $\Delta E/E \sim 2 \times 10^{-5}$  for a strain of  $4.1 \times 10^{-5}$ . This causes  $\Delta R/R$  to have the shape of the derivative of a peaked function, i.e., a positive peak followed by a negative peak, with a zero at the surface plasmon frequency. The negative peak probably cannot be seen on the shoulder of the large peak due to the interband transition, but there is some weak positive structure in  $\Delta R/R$  below the surface plasmon frequency. When Green<sup>30</sup> alloyed silver with 5% zinc or cadmium, the 3.5-eV peak in  $\epsilon_2$  disappeared. There are two reasons for this disappearance. The surface plasmons damp out upon alloying,<sup>7</sup> and the strong  $L_3 \rightarrow L_{2'}$  transition obscures their presence. Thus we expect that the low-energy structure in  $\Delta R/R$  and  $\Delta\epsilon_2$  for most of our alloy samples does not arise from a surface effect, as probably is the case for silver, but from interband transitions.

Normally in pure metals one does not consider indirect transitions, but this is not the case for alloys. The addition of indium to silver increases the probability of indirect transitions. The indium atoms provide the scattering mechanism necessary to conserve momentum in an indirect transition. Ziman<sup>36</sup> derived an approximate expression giving the ratio of indirect to direct transitions in alloys. From this expression it was found that the indirect transitions should be as strong as the direct transitions for the 3.3 and 5.0% alloys. Therefore, the onset of structure in  $\Delta\epsilon_2$  for the alloys probably denotes the (Fermi level)  $\rightarrow L_1$  indirect energy gap (with due allowances for lifetime broadening) and not the energy of the lowest allowed direct transition.

As was done for silver, the  $L$  band gap for the alloys can be estimated from the structure in  $\Delta\epsilon_2$ . We believe that the  $L$  band gaps for the alloys, in order of increasing

concentration, are 4.10, 4.0, 3.9, and about 3.7–3.8 eV. In the 0.4% alloy, the  $L$  band-gap energy was chosen to be that of the zero in  $\Delta\epsilon_2$ . In the more concentrated alloys, the choice becomes more ambiguous because of the structure due to indirect transitions and the general broadening. We have chosen energies slightly below those of the zeros in  $\Delta\epsilon_2$ .

On the right side of Fig. 10 is a tentative partial band structure for the 5% In alloy. We have set the  $L$  band gap equal to 3.75 eV, probably correct to within 0.05 eV. It was assumed that each indium atom contributed three electrons to the conduction band. The shift of the Fermi level with respect to the bottom of the conduction band was calculated from the electronic specific heat of silver.<sup>37</sup> The effects of alloying on the electronic specific heat are small and the value for silver can be used for our alloys. ML reported  $L_{2'} \rightarrow L_1$  band gaps of 4.24 and 3.82 eV for silver and Ag+4.1 at.% In, respectively, although the value for pure silver was an estimate of others.<sup>24</sup> We believe that the value 4.15 eV for silver is better. By plotting the gap energies for our alloys versus indium concentration, a straight line can be placed through the points, if 0.05-eV error is assigned the last two alloys, and 3.80 eV is the interpolated gap for 4.1 at.% indium. Other differences between Fig. 11 of ML and our Fig. 10 arise from different relative curvatures assumed for the two conduction bands. The theory of Cohen and Heine<sup>38</sup> gives a poor value for the  $L_{2'} \rightarrow L_1$  band gap in silver, but, as ML mention, the shift of this gap energy upon alloying is given quite well. For 5% indium in silver, their theory gives a gap decrease of 0.51 eV, while we find a value of about 0.40 eV.

From Fig. 10 it is apparent that if only direct transitions were possible in the alloys, the energy interval from the  $L$  band gap to the onset of structure in  $\Delta\epsilon_2$  would be less than 0.2 eV, ignoring broadening. For the alloys, this energy is about 0.6–0.7 eV, strongly suggesting that indirect transitions contribute to the structure in the alloys. The increase in the low-energy structure in  $\Delta\epsilon_2$  with increasing indium concentration is attributed largely to the increase in indirect transitions, which grow from zero in silver to about the same strength as direct transitions in the 5% alloy. To a lesser extent direct transitions contribute to the increase in  $\Delta\epsilon_2$  at low energy as the states farther from  $L_{2'}$  become occupied upon alloying.

#### ACKNOWLEDGMENT

We would like to thank Professor C. A. Swenson for suggesting that the data of Ref. 19 could be used to estimate  $d \ln r / d \ln V$  for the alloys.

<sup>35</sup> P. A. Fedders, Phys. Rev. **165**, 580 (1968).

<sup>36</sup> J. M. Ziman, Phil. Mag. **5**, 757 (1960).

<sup>37</sup> B. A. Green and H. U. Cuthbert, Phys. Rev. **137**, A1168 (1965).

<sup>38</sup> M. H. Cohen and V. Heine, Advan. Phys. **7**, 395 (1958).